

# Passivity-based Visual Motion Observer with Panoramic Camera for Pose Control

Hiroyuki Kawai · Toshiyuki Murao ·  
Masayuki Fujita

Received: date / Accepted: date

**Abstract** This paper considers the vision-based estimation and pose control with a panoramic camera via passivity approach. First, a hyperbolic projection of a panoramic camera is presented. Next, using standard body-attached coordinate frames (the world frame, mirror frame, camera frame and object frame), we represent the body velocity of the relative rigid body motion (position and orientation). After that, we propose a visual motion observer to estimate the relative rigid body motion from the measured camera data. We show that the estimation error system with a panoramic camera has the passivity which allows us to prove stability in the sense of Lyapunov. The visual motion error system which consists of the estimation error system and the pose control error system preserves the passivity. After that, stability and  $L_2$ -gain performance analysis for the closed-loop system are discussed via Lyapunov method and dissipative systems theory, respectively. Finally, simulation and experimental results are shown in order to confirm the proposed method.

**Keywords** Visual Feedback Control · Panoramic Camera · Passivity · Lyapunov Stability

## 1 Introduction

Vision gives us rich information in order to respond to surrounding motions. Mechanical systems also need many information in an efficient manner autonomously. The

---

H. Kawai  
Department of Robotics, Kanazawa Institute of Technology, Ishikawa, Japan  
E-mail: hiroyuki@neptune.kanazawa-it.ac.jp

T. Murao  
Master Program of Innovation for Design and Engineering, Advanced Institute of Industrial Technology, Tokyo, Japan  
E-mail: murao-toshiyuki@aiit.ac.jp

M. Fujita  
Department of Mechanical and Control Engineering, Tokyo Institute of Technology, Tokyo, Japan  
E-mail: fujita@ctrl.titech.ac.jp

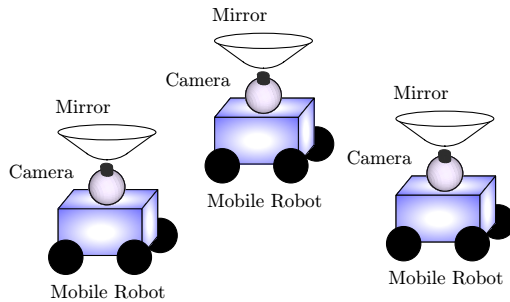


**Fig. 1** Omnidirectional vision-based formation of mobile robots.

combination of mechanical control with visual information, so-called visual feedback control or visual servoing, is important when we consider a mechanical system working under dynamical environments [1]. Recently, Lippiello *et al.* [2] presented a position-based visual servoing for a hybrid eye-in-hand/eye-to-hand multicamera configuration by using the extended Kalman filter and a multiarm robotic cell. Gans and Hutchinson [3] proposed hybrid switched-system control which utilizes image-based and position-based visual feedback control. Hu *et al.* [4] considered homography-based robust visual servo control for the uncertainty of the camera calibration. In our previous works, we discussed dynamic visual feedback control for 3D target tracking based on passivity [5]–[7]. Although these previous works give us the new vision-based robot control theory systematically, most of the works use a simple perspective projection by a pinhole camera. Thus, it was implicitly supposed that the target object exists on the direction of the optical center of the camera.

On the other hand, omnidirectional cameras are useful for recognizing unknown surroundings widely. Geyer and Daniilidis [8] presented a unifying theory for all central panoramic systems, i.e., an equivalence of catadioptric and spherical projections. Hadj-Abdelkader *et al.* [9] proposed a catadioptric image-based control strategy for nonholonomic robot in order to follow a 3D line. Mariottini *et al.* [10] reviewed the several epipolar geometry estimation algorithms by using an omnidirectional camera and gave us Epipolar Geometry Toolbox which is a simulation environment with MATLAB. Fomena and Chaumette [11] considered improvements on modeling features for visual servoing using a spherical projection. However, the relative pose between the robot and the target object can not be obtained except at the desired pose, while the pose of a robot with a panoramic camera coincides with a desired one in these methods. For the vision-based formation control of mobile robots with central panoramic cameras, Das *et al.* [12] discussed cooperative control of a group of nonholonomic mobile robots by using an extended Kalman filter-based estimation algorithm. Vidal *et al.* [13] used motion segmentation techniques to estimate the position of each leader. However, stability analysis have not been discussed for both pose control and pose estimation in these works which dealt with the pose control by using a panoramic camera, while practical methods have been proposed for the set point control problem. Although the vision-based pose synchronization has been proposed in our previous work [14], a perspective projection model of a pinhole camera is used in order to the estimate relative pose.

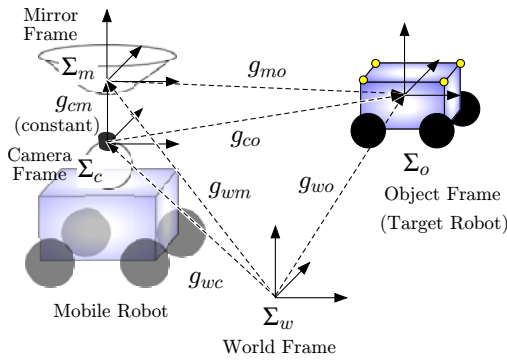


**Fig. 2** Coordinate frames for mobile robots.

This paper deals with visual motion observer by using a panoramic camera for pose control of mobile robot systems as depicted in Fig. 1. The advantage of our proposed method is that the relative pose between the leader and the follower robot can be obtained by using a single panoramic camera in the around direction. Moreover, a desired pose between the leader and the follower robot can be given directly, while our proposed method does not need a desired image a priori. The estimation error system with a panoramic camera has the passivity which allows us to prove stability in the sense of Lyapunov. The visual motion error system which consists of the estimation error system and the pose control error system preserves the passivity. After that, stability and  $L_2$ -gain performance analysis for the closed-loop system are discussed. In the proposed control law, we can design both the estimation and the control gain independently in the same framework. Finally, simulation and experimental results are shown in order to confirm the proposed method.

## 2 Panoramic Camera

In our previous works [5]–[7], it was implicitly supposed that the target object existed on the direction of the optical center of the camera. It was reported that there existed a case of missing a target object in the position-based visual servoing [15]. In order to catch the leader robot in the whole space where the controlled follower robot will move, we use a panoramic camera instead of a simple pinhole camera. Hereafter, the leader and the follower robot are regarded as a target object and a controlled robot which has a panoramic camera, respectively, as shown in Fig. 2

Visual feedback systems by using a panoramic camera use four coordinate frames which consist of a world frame  $\Sigma_w$ , a mirror frame  $\Sigma_m$ , a camera frame  $\Sigma_c$ , and an object frame  $\Sigma_o$  as in Fig. 2. Let  $p_{mo} \in \mathcal{R}^3$  and  $e^{\hat{\xi}\theta_{mo}} \in SO(3)$  be the position vector and the rotation matrix from the mirror frame  $\Sigma_m$  to the object frame  $\Sigma_o$ . Then, the relative rigid body motion (position and orientation) from  $\Sigma_m$  to  $\Sigma_o$  can be represented by  $g_{mo} = (p_{mo}, e^{\hat{\xi}\theta_{mo}}) \in SE(3)$ <sup>1</sup>. Similarly,  $g_{wm} = (p_{wm}, e^{\hat{\xi}\theta_{wm}})$ ,  $g_{wc} = (p_{wc}, e^{\hat{\xi}\theta_{wc}})$  and  $g_{wo} = (p_{wo}, e^{\hat{\xi}\theta_{wo}})$  denote the rigid body motions from the world frame  $\Sigma_w$  to

<sup>1</sup> The notation of the homogeneous transform is denoted in Appendix A



From Fig. 3, the relation between the camera frame  $\Sigma_c$  and the mirror frame  $\Sigma_m$  can be represented as

$$p_{cm} = \begin{bmatrix} 0 \\ 0 \\ 2r \end{bmatrix} e^{\hat{\xi}\theta_{cm}} = I_3 \quad (3)$$

and it is assumed that these parameters are known. Moreover,  $p_{mh}$  can be represented as follows:

$$p_{mh} = \alpha p_{mo} \quad (0 < \alpha < 1) \quad (4)$$

Because  $\alpha p_{mo}$  has to satisfy the constraint (1), the following relation holds

$$\frac{(\alpha z_{mo} + r)^2}{a^2} - \frac{\alpha^2 x_{mo}^2 + \alpha^2 y_{mo}^2}{b^2} = 1. \quad (5)$$

Solving Eq. (5) for  $\alpha$ , we obtain

$$\alpha(p_{mo}) = \frac{b^2(rz_{mo} + a\|p_{mo}\|)}{a^2x_{mo}^2 + a^2y_{mo}^2 - b^2z_{mo}^2} \quad (6)$$

where  $\alpha(p_{mo})$  represents that  $\alpha$  depends on  $p_{mo}$  explicitly.

From Eqs. (2)(3) and  $z_{ch} = z_{cm} + z_{mh} = 2r + \alpha(p_{mo})z_{mo}$ , the hyperbolic projection of the panoramic camera can be represented as

$$s = A \frac{1}{2r + \alpha(p_{mo})z_{mo}} (\alpha(p_{mo})p_{mo} + p_{cm}) \quad (7)$$

where we exploit the composition rule [16], i.e.,  $p_{ch} = e^{\hat{\xi}\theta_{cm}}p_{mh} + p_{cm}$ .

## 2.2 Image Feature for Panoramic Camera

In order to know the relative rigid body motion  $g_{mo}$  from the visual information, we consider the feature points on the rigid target object<sup>2</sup>. From the hyperbolic projection of the panoramic camera, we consider the obtainable visual information.

Let  $p_{oi} \in \mathcal{R}^3$  and  $p_{mi} \in \mathcal{R}^3$  be the position vectors of the target object's  $i$ -th feature points ( $i = 1, \dots, n$ , ( $n \geq 4$ )) relative to  $\Sigma_o$  and  $\Sigma_m$ , respectively (see Fig. 4). Using a transformation of the coordinates, we have

$$p_{mi} = g_{mo}p_{oi} \quad (8)$$

where  $p_{mi}$  and  $p_{oi}$  should be regarded, with a slight abuse of notation, as  $[p_{mi}^T \ 1]^T$  and  $[p_{oi}^T \ 1]^T$  via the well-known homogeneous coordinate representation in robotics, respectively (see, e.g., [16]).

The hyperbolic projection of the  $i$ -th feature point onto the image plane gives us the image plane coordinate  $f_i := [f_{xi} \ f_{yi}]^T \in \mathcal{R}^2$  as

$$f_i = \frac{\lambda\alpha(p_{mi})}{2r + \alpha(p_{mi})z_{mi}} \begin{bmatrix} x_{mi} \\ y_{mi} \end{bmatrix} \quad (9)$$

<sup>2</sup> The feature points on the rigid object are suitable for the estimation of the position and the orientation in 3D workspace.

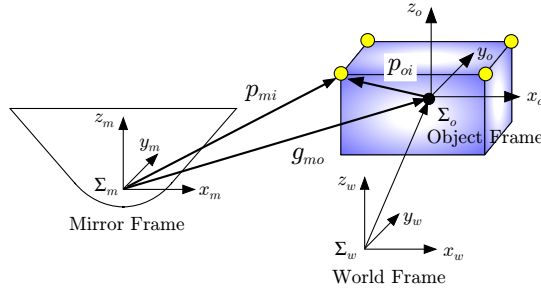


**Fig. 4** Feature points on target object.

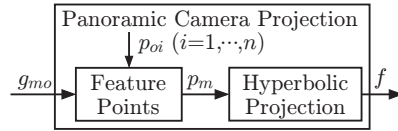


**Fig. 5** Block diagram of panoramic camera projection.

where  $\alpha(p_{mi})$  means that  $p_{mo}$  in Eq. (6) is replaced with  $p_{mi} = [x_{mi} \ y_{mi} \ z_{mi}]^T$ . It is straightforward to extend this model to  $n$  image points by simply stacking the vectors of the image plane coordinate, i.e.,

$$f(g_{mo}) := [f_1^T \ \dots \ f_n^T]^T \in \mathcal{R}^{2n} \quad (10)$$

and  $p_m := [p_{m1}^T \ \dots \ p_{mn}^T]^T \in \mathcal{R}^{3n}$ . We assume that multiple feature points on a known object are given. Although the problem of extracting the feature points from the target object is interesting in its own right, we will not focus on this problem and merely assume that the image feature are obtained by well-known techniques. From Eq. (8) and Fig. 5 which shows the block diagram of the panoramic camera projection, the image feature  $f$  only depends on the relative rigid body motion  $g_{mo}$ .

### 2.3 Body Velocity for Panoramic Camera

The relative rigid body motion  $g_{mo}$  is discussed in this section, because the image feature  $f$  only depends on  $g_{mo}$ . We recall that visual feedback systems by using a panoramic camera use four coordinate frames and the relative rigid body motion from  $\Sigma_m$  to  $\Sigma_o$  can be represented by  $g_{mo} = (p_{mo}, e^{\hat{\xi}\theta_{mo}})$  as shown in Fig. 2.

The relative rigid body motion from  $\Sigma_m$  to  $\Sigma_o$  can be led by using the composition rule for rigid body transformations as follows:

$$g_{mo} = g_{wm}^{-1} g_{wo}. \quad (11)$$

The relative rigid body motion involves the velocity of each rigid body. To this aid, let us consider the velocity of a rigid body as described in [16]. We define the body velocity of the mirror relative to the world frame  $\Sigma_w$  as  $V_{wm}^b = [v_{wm}^T \ \omega_{wm}^T]^T$ , where  $v_{wm}$  and  $\omega_{wm}$  represent the velocity of the origin and the angular velocity from  $\Sigma_w$  to  $\Sigma_m$ , respectively.

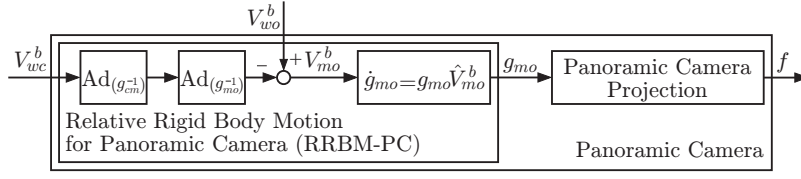


**Fig. 6** Block diagram of panoramic camera which consists of relative rigid body motion and panoramic camera projection.

Differentiating Eq. (11) with respect to time, the body velocity of the relative rigid body motion  $g_{mo}$  can be written as follows (See [6]):

$$V_{mo}^b = -\text{Ad}_{(g_{mo}^{-1})} V_{wm}^b + V_{wo}^b \quad (12)$$

where  $V_{wo}^b$  is the body velocity of the target object relative to  $\Sigma_w$ . Because the camera velocity  $V_{wc}^b$  is adequate as an input rather than the mirror velocity  $V_{wm}^b$  in this framework, we lead the body velocity of the relative rigid body motion with the camera velocity.

The body velocity of the mirror frame relative to  $\Sigma_w$  will be denoted as

$$\hat{V}_{wm}^b = g_{wm}^{-1} \dot{g}_{wm} = g_{wm}^{-1} \dot{g}_{wc} g_{cm} = g_{wm}^{-1} \dot{g}_{wc} g_{cm}^{-1} \dot{g}_{wc} g_{cm} = g_{cm}^{-1} \hat{V}_{wc}^b g_{cm}. \quad (13)$$

From the property concerning the adjoint transformation,  $V_{wm}^b$  can be transformed into

$$V_{wm}^b = \text{Ad}_{(g_{cm}^{-1})} V_{wc}^b. \quad (14)$$

Thus, Eq. (12) can be transformed into

$$V_{mo}^b = -\text{Ad}_{(g_{mo}^{-1})} \text{Ad}_{(g_{cm}^{-1})} V_{wc}^b + V_{wo}^b. \quad (15)$$

This is the body velocity of the relative rigid body motion for the panoramic camera. While  $g_{cm}$  is known information from Eq. (3),  $g_{mo}$  and  $g_{wo}$ , i.e.,  $V_{mo}^b$  and  $V_{wo}^b$ , are unknown information in the visual feedback system. Fig. 6 shows the block diagram of the panoramic camera which consists of the relative rigid body motion and the panoramic camera projection. Then, the control objective is described as follows.

*Control Objective:* The controlled mobile robot follows the target robot, i.e., the relative rigid body motion  $g_{co}$  is coincided with the desired one  $g_d$ .

Because  $g_{cm}$  is known a priori,  $g_{co}$  can be obtained from  $g_{mo}$  by the composition rule  $g_{co} = g_{cm} g_{mo}$ . Thus, we consider the estimate of  $g_{mo}$  for the above control objective.

### 3 Visual Motion Observer

In this section, we propose a visual motion observer by using a single panoramic camera in order to estimate the relative rigid body motion from the mirror frame to the object frame.

### 3.1 Image Jacobian for Panoramic Camera

Since the measurable information is only the image feature  $f$  from the panoramic camera, we consider a visual motion observer in order to estimate the relative rigid body motion  $g_{mo}$  from the image feature  $f$ . Using the body velocity of the relative rigid body motion (15), we choose estimates  $\bar{g}_{mo} = (\bar{p}_{mo}, e^{\hat{\xi}_{\bar{\theta}_{mo}}})$  and  $\bar{V}_{mo}^b$  of the relative rigid body motion and velocity, respectively as

$$\bar{V}_{mo}^b = -\text{Ad}_{(\bar{g}_{mo}^{-1})} \text{Ad}_{(g_{cm}^{-1})} V_{wc}^b + u_e. \quad (16)$$

The new input  $u_e = [v_{ue}^T \ \omega_{ue}^T]^T$  is to be determined in order to drive the estimated values  $\bar{g}_{mo}$  and  $\bar{V}_{mo}^b$  to their actual ones.

Similarly to Eqs. (8) and (9), the estimated image feature  $\bar{f}_i$  ( $i = 1, \dots, n$ ) is defined as

$$\bar{p}_{mi} = \bar{g}_{mo} p_{oi} \quad (17)$$

$$\bar{f}_i = \frac{\lambda \alpha(\bar{p}_{mi})}{2r + \alpha(\bar{p}_{mi}) \bar{z}_{mi}} \begin{bmatrix} \bar{x}_{mi} \\ \bar{y}_{mi} \end{bmatrix} \quad (18)$$

where  $\bar{p}_{mi} := [\bar{x}_{mi} \ \bar{y}_{mi} \ \bar{z}_{mi}]^T$ .  $\bar{f}(\bar{g}_{mo}) := [\bar{f}_1^T \ \dots \ \bar{f}_n^T]^T \in \mathcal{R}^{2n}$  means the  $n$  image points case.

In order to establish the estimation error system, we define the estimation error between the estimated value  $\bar{g}_{mo}$  and the actual relative rigid body motion  $g_{mo}$  as

$$g_{ee} := \bar{g}_{mo}^{-1} g_{mo} \quad (19)$$

in other words,  $p_{ee} = e^{-\hat{\xi}_{\bar{\theta}_{mo}}}(p_{mo} - \bar{p}_{mo})$  and  $e^{\hat{\xi}_{\theta_{ee}}} = e^{-\hat{\xi}_{\bar{\theta}_{mo}}} e^{\hat{\xi}_{\theta_{mo}}}$ . Note that  $p_{mo} = \bar{p}_{mo}$  and  $e^{\hat{\xi}_{\theta_{mo}}} = e^{\hat{\xi}_{\bar{\theta}_{mo}}}$  if and only if  $g_{ee} = I_4$ , i.e.,  $p_{ee} = 0$  and  $e^{\hat{\xi}_{\theta_{ee}}} = I_3$ . We next define the error vector of the rotation matrix  $e^{\hat{\xi}_{\theta_{ab}}}$  as

$$e_R(e^{\hat{\xi}_{\theta_{ab}}}) := \text{sk}(e^{\hat{\xi}_{\theta_{ab}}})^\vee \quad (20)$$

where  $\text{sk}(e^{\hat{\xi}_{\theta_{ab}}})$  denotes  $\frac{1}{2}(e^{\hat{\xi}_{\theta_{ab}}} - e^{-\hat{\xi}_{\theta_{ab}}})$ . Using this notation, the vector of the estimation error is given by

$$e_e := \begin{bmatrix} p_{ee}^T \\ e_R^T(e^{\hat{\xi}_{\theta_{ee}}}) \end{bmatrix}^T. \quad (21)$$

From the above, we derive a relation between the actual and the estimated image feature. Suppose the attitude estimation error  $\theta_{ee}$  is small enough that we can let  $e^{\hat{\xi}_{\theta_{ee}}} \simeq I + \text{sk}(e^{\hat{\xi}_{\theta_{ee}}})$ . Then we have the following relation between the actual feature point  $p_{mi}$  and the estimated one  $\bar{p}_{mi}$

$$p_{mi} - \bar{p}_{mi} = e^{\hat{\xi}_{\bar{\theta}_{mo}}} [I - \hat{p}_{oi}] \begin{bmatrix} p_{ee} \\ e_R(e^{\hat{\xi}_{\theta_{ee}}}) \end{bmatrix}. \quad (22)$$

Using a first-order Taylor expansion approximation, the relation between the actual image feature and the estimated one can be expressed as

$$f_i - \bar{f}_i = \left[ \frac{\partial f_i}{\partial x_{mi}} \Big|_{p_{mi}=\bar{p}_{mi}} \quad \frac{\partial f_i}{\partial y_{mi}} \Big|_{p_{mi}=\bar{p}_{mi}} \quad \frac{\partial f_i}{\partial z_{mi}} \Big|_{p_{mi}=\bar{p}_{mi}} \right] (p_{mi} - \bar{p}_{mi}) \quad (23)$$

where the partial differentiations  $\partial f_i/\partial x_{mi}$ ,  $\partial f_i/\partial y_{mi}$  and  $\partial f_i/\partial z_{mi}$  are represented as follows.

$$\frac{\partial f_i}{\partial x_{mi}} = \frac{2r\lambda\alpha_x(p_{mi})}{(2r + \alpha(p_{mi})z_{mi})^2} \begin{bmatrix} x_{mi} \\ y_{mi} \end{bmatrix} + \frac{\lambda\alpha(p_{mi})}{2r + \alpha(p_{mi})z_{mi}} \begin{bmatrix} 1 \\ 0 \end{bmatrix} \quad (24)$$

$$\frac{\partial f_i}{\partial y_{mi}} = \frac{2r\lambda\alpha_y(p_{mi})}{(2r + \alpha(p_{mi})z_{mi})^2} \begin{bmatrix} x_{mi} \\ y_{mi} \end{bmatrix} + \frac{\lambda\alpha(p_{mi})}{2r + \alpha(p_{mi})z_{mi}} \begin{bmatrix} 0 \\ 1 \end{bmatrix} \quad (25)$$

$$\frac{\partial f_i}{\partial z_{mi}} = \frac{2r\lambda\alpha_z(p_{mi})}{(2r + \alpha(p_{mi})z_{mi})^2} \begin{bmatrix} x_{mi} \\ y_{mi} \end{bmatrix} - \frac{\lambda\alpha^2(p_{mi})}{(2r + \alpha(p_{mi})z_{mi})^2} \begin{bmatrix} x_{mi} \\ y_{mi} \end{bmatrix} \quad (26)$$

where

$$\begin{aligned} \alpha_x(p_{mi}) &= \frac{\partial\alpha(p_{mi})}{\partial x_{mi}} = \frac{-2a^2b^2rx_{mi}z_{mi}\|p_{mi}\| - ab^2x_{mi}(r^2z_{mi}^2 + a^2\|p_{mi}\|^2)}{(a^2x_{mi}^2 + a^2y_{mi}^2 - b^2z_{mi}^2)^2\|p_{mi}\|} \\ \alpha_y(p_{mi}) &= \frac{\partial\alpha(p_{mi})}{\partial y_{mi}} = \frac{-2a^2b^2ry_{mi}z_{mi}\|p_{mi}\| - ab^2y_{mi}(r^2z_{mi}^2 + a^2\|p_{mi}\|^2)}{(a^2x_{mi}^2 + a^2y_{mi}^2 - b^2z_{mi}^2)^2\|p_{mi}\|} \\ \alpha_z(p_{mi}) &= \frac{\partial\alpha(p_{mi})}{\partial z_{mi}} = \frac{ab^2z_{mi}(r^2(x_{mi}^2 + y_{mi}^2) + b^2\|p_{mi}\|^2)}{(a^2x_{mi}^2 + a^2y_{mi}^2 - b^2z_{mi}^2)^2\|p_{mi}\|} \\ &\quad + \frac{b^2r(b^2z_{mi}^2 + a^2x_{mi}^2 + a^2y_{mi}^2)\|p_{mi}\|}{(a^2x_{mi}^2 + a^2y_{mi}^2 - b^2z_{mi}^2)^2\|p_{mi}\|}. \end{aligned}$$

Let us define the image feature error as  $f_e := f(g_{mo}) - \bar{f}(\bar{g}_{mo})$ . Hence, the relation between the actual image feature and the estimated one can be given by

$$f_e = J(\bar{g}_{mo})e_e, \quad (27)$$

where  $J(\bar{g}_{mo}) : SE(3) \rightarrow \mathcal{R}^{2n \times 6}$  is defined as

$$J(\bar{g}_{mo}) := [J_1^T(\bar{g}_{mo}) \ J_2^T(\bar{g}_{mo}) \ \cdots \ J_n^T(\bar{g}_{mo})]^T \quad (28)$$

$$\begin{aligned} J_i(\bar{g}_{mo}) &:= \left[ \frac{\partial f_i}{\partial x_{mi}} \Big|_{p_{mi}=\bar{p}_{mi}} \quad \frac{\partial f_i}{\partial y_{mi}} \Big|_{p_{mi}=\bar{p}_{mi}} \quad \frac{\partial f_i}{\partial z_{mi}} \Big|_{p_{mi}=\bar{p}_{mi}} \right] \times e^{\hat{\xi}_{\bar{g}_{mo}}} [I - \hat{p}_{oi}]. \\ &\quad (i = 1, \dots, n) \quad (29) \end{aligned}$$

We assume that the matrix  $J(\bar{g}_{mo})$  is full column rank for all  $\bar{g}_{mo} \in SE(3)$ . Then, the relative rigid body motion can be uniquely defined by the image feature vector. Because this may not hold in some cases when  $n = 3$ , it is known that  $n \geq 4$  is desirable for the full column rank of the image Jacobian [17].

The above discussion shows that we can derive the vector of the estimation error  $e_e$  from image feature  $f$  and the estimated value of the relative rigid body motion  $\bar{g}_{mo}$ ,

$$e_e = J^\dagger(\bar{g}_{mo})f_e \quad (30)$$

where  $\dagger$  denotes the pseudo-inverse. Fig. 7 shows the relation between the image feature error  $f_e$  and the estimation error  $e_e$ . Therefore the estimation error  $e_e$  can be exploited in the visual feedback control law using image feature  $f$  obtained from the panoramic camera.

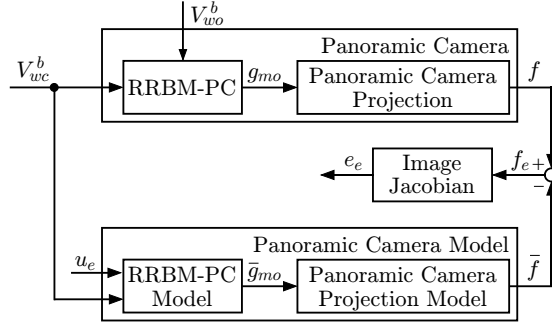


**Fig. 7** Block diagram of estimation error vector obtained from panoramic camera and panoramic camera model.

*Remark 1* If we select one and the imaginary unit as  $a$  and  $b$  numerically, i.e.,  $a = 1$ ,  $b = i$ , then the image Jacobian for the panoramic camera (29) equals to the pinhole's one [6] as follows:  $\frac{\partial f_i}{\partial x_{mi}} = \frac{\lambda}{z_{mi}} [1 \ 0]^T$ ,  $\frac{\partial f_i}{\partial y_{mi}} = \frac{\lambda}{z_{mi}} [0 \ 1]^T$ ,  $\frac{\partial f_i}{\partial z_{mi}} = -\frac{\lambda}{z_{mi}^2} [x_{mi} \ y_{mi}]^T$ . Thus our previous work [6] can be regarded as a special case of this study, although the pinhole camera has different applications from the panoramic one in the practical point of view.

### 3.2 Passivity of Estimation Error System

In the same way as Eq. (12), the estimation error system can be represented by

$$V_{ee}^b = -\text{Ad}_{(g_{ee}^{-1})} u_e + V_{wo}^b. \quad (31)$$

Then, we have the following lemma relating the input  $u_e$  to the vector form of the estimation error  $e_e$ .

**Lemma 1** *If  $V_{wo}^b = 0$ , then the following inequality holds for the estimation error system (31).*

$$\int_0^T u_e^T (-e_e) dt \geq -\beta_e \quad (32)$$

where  $\beta_e$  is a positive scalar.

*Proof* Consider the positive definite function

$$V_e = \frac{1}{2} \|p_{ee}\|^2 + \phi(e^{\hat{\xi}\theta_{ee}}) \quad (33)$$

where  $\phi(e^{\hat{\xi}\theta_{ab}}) := \frac{1}{2} \text{tr}(I - e^{\hat{\xi}\theta_{ab}})$  is the error function of the rotation matrix [18]. Evaluating the time derivative of  $V_e$  along the trajectories of Eq. (31) gives us

$$\begin{aligned} \dot{V}_e &= p_{ee}^T e^{\hat{\xi}\theta_{ee}} e^{-\hat{\xi}\theta_{ee}} \dot{p}_{ee} + e_R^T(e^{\hat{\xi}\theta_{ee}}) e^{\hat{\xi}\theta_{ee}} \omega_{ee} \\ &= e_e^T \text{Ad}_{(e^{\hat{\xi}\theta_{ee}})} V_{ee}^b = -e_e^T u_e - p_{ee}^T \hat{\omega}_{ue} p_{ee} \\ &= u_e^T (-e_e). \end{aligned} \quad (34)$$

Integrating Eq. (34) from 0 to  $T$  yields

$$\int_0^T u_e^T (-e_e) d\tau = \int_0^T \dot{V} d\tau \geq -V(0) \geq -\beta_e \quad (35)$$

where  $\beta_e$  is the positive scalar which only depends on the initial state of  $g_{ee}$ .

*Remark 2* Let us consider the vector form of the estimation error  $-e_e$  as its output. Then, Lemma 1 says that the estimation error system (31) is *passive* from the input  $u_e$  to the output  $-e_e$ . In fact, the body velocity of the relative rigid body motion (15) has passivity, the estimation error system preserves its passivity.

### 3.3 Stability Analysis of Visual Motion Observer

Based on the above passivity property of the estimation error system, we consider the following control law.

$$u_e = K_e e_e \quad (36)$$

where  $K_e := \text{diag}\{k_{e1}, \dots, k_{e6}\}$  is the positive gain matrix of  $x$ ,  $y$  and  $z$  axes of the translation and the rotation for the estimation error.

**Theorem 1** *If  $V_{wo}^b = 0$ , then the equilibrium point  $e_e = 0$  for the closed-loop system (31) and (36) is asymptotic stable.*

*Proof* In the proof of Lemma 1, we have already shown that the time derivative of  $V_e$  along the trajectory of the system (31) is formulated as Eq. (34). Using the control input (36), Eq. (34) can be transformed into

$$\dot{V}_e = -e_e^T K_e e_e. \quad (37)$$

This completes the proof.

It should be noted that if the vector of the estimation error is equal to zero, then the estimated relative rigid body motion  $\bar{g}_{mo}$  equals the actual one  $g_{mo}$ . Fig. 8 shows a block diagram of the visual motion observer with a panoramic camera. By the proposed visual motion observer, the unmeasurable motion  $g_{co}$  will be exploited as the part of the control law. The relative pose between the robot and the target object can be obtained by using a single panoramic camera in the around direction. This is the advantage of our proposed method. Our proposed visual motion observer is composed just as the Luenberger observer for linear systems.

*Remark 3* The estimation error vector is configured by available information (i.e., the measurement and the estimate) though it is defined by unavailable one. This is one of the main contributions of this paper.

## 4 Visual Motion Observer-based Pose Control

Let us consider the dual of the estimation error system, which we call the pose control error system, in order to achieve the control objective in this section.

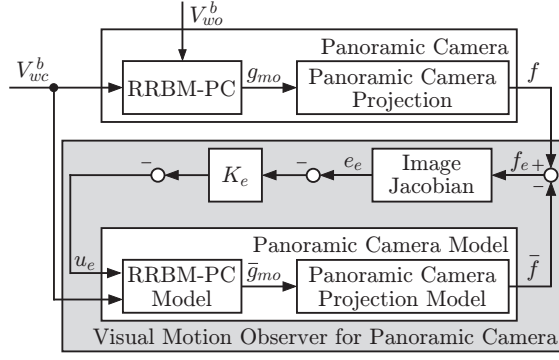


Fig. 8 Block diagram of visual motion observer.

#### 4.1 Pose Control Error System

In previous work [6], we defined the pose control error as  $g_{ec} = g_d^{-1} \bar{g}_{co}$ , which represents the error between the estimated value  $\bar{g}_{co}$  and the reference of the relative rigid body motion  $g_d$ . However, the estimation input  $u_e$  has affected directly the camera control error system, because the pose control error was defined using the estimated value  $\bar{g}_{co}$ . This has deteriorated the performance of the estimation in the visual feedback control. In this paper, we define the pose control error as follows:

$$g_{ec} = g_d^{-1} g_{co}, \quad (38)$$

which represents the error between the relative rigid body motion  $g_{co}$  and the reference one  $g_d$ . By using the above pose control error (38), we can construct the pose control error system in order to overcome the deterioration of the estimation.

Next, we have to derive the pose control error  $g_{ec}$  without non-measurable value  $g_{co}$  in order to use it in a control law. Using the composition rule, the pose control error  $g_{ec}$  can be transformed as

$$g_{ec} = g_d^{-1} g_{co} = g_d^{-1} g_{cm} g_{mo} = g_d^{-1} g_{cm} \bar{g}_{mo} \bar{g}_{mo}^{-1} g_{mo} = g_d^{-1} g_{cm} \bar{g}_{mo} g_{ee}. \quad (39)$$

In Eq. (39),  $g_d$ ,  $g_{cm}$  and  $\bar{g}_{mo}$  are available information. While the estimation error vector  $e_e$  can be obtained as Eq. (30), the estimation error matrix  $g_{ee}$ , which is defined using non-measurable value  $g_{mo}$  as Eq. (19), cannot be utilized directly.

Focusing on the definition of the estimation error vector  $e_e$ , i.e.,  $e_e = [p_{ee}^T e_R^T(e^{\hat{\xi}\theta_{ee}})]^T$ , the position estimation error  $p_{ee}$  can be given directly from  $e_e$ . As for to the rotation estimation error  $e^{\hat{\xi}\theta_{ee}}$ , if we assume that the region of the attitude estimation error is restricted to  $-\frac{\pi}{2} \leq \theta_{ee} \leq \frac{\pi}{2}$ , then  $\xi\theta_{ee}$  can be gained by

$$\xi\theta_{ee} = \frac{\sin^{-1} \|e_R(e^{\hat{\xi}\theta_{ee}})\|}{\|e_R(e^{\hat{\xi}\theta_{ee}})\|} e_R(e^{\hat{\xi}\theta_{ee}}). \quad (40)$$

Thus it is possible to obtain the pose control error  $g_{ec}$  from the available information by Eq. (39), since  $g_{ee}$  can be derived from  $e_e$  through  $\xi\theta_{ee}$ . Here, it should be noted that the assumption  $-\frac{\pi}{2} \leq \theta_{ee} \leq \frac{\pi}{2}$  will not be a new constraint, since we have already set

the assumption that the attitude estimation error  $\theta_{ee}$  is small enough in Section 3.1. Using the notation  $e_R(e^{\hat{\xi}\theta})$ , the vector of the pose control error is defined as

$$e_c := \begin{bmatrix} p_{ec}^T & e_R^T(e^{\hat{\xi}\theta_{ec}}) \end{bmatrix}^T. \quad (41)$$

Note that  $e_c = 0$  iff  $p_{ec} = 0$  and  $e^{\hat{\xi}\theta_{ec}} = I_3$ .

The reference of the relative rigid body motion  $g_d$  is assumed to be constant in this paper, i.e.,  $\dot{g}_d = 0$  and hence  $V_{ec}^b = V_{co}^b$ . Thus, the pose control error system can be represented as

$$V_{ec}^b = -\text{Ad}_{(g_{ec}^{-1})} \left( \text{Ad}_{(g_d^{-1})} V_{wc}^b \right) + V_{wo}^b. \quad (42)$$

This is dual to the estimation error system (31). Similar to the estimation error system, the pose control error system also preserves the passivity property.

#### 4.2 Passivity of Visual Motion Error System

Combining the estimation error system (31) and the pose control one (42), we construct the visual motion observer-based pose control error system (we call the visual motion error system) as follows:

$$\begin{bmatrix} V_{ec}^b \\ V_{ee}^b \end{bmatrix} = \begin{bmatrix} -\text{Ad}_{(g_{ec}^{-1})} & 0 \\ 0 & -\text{Ad}_{(g_{ee}^{-1})} \end{bmatrix} u + \begin{bmatrix} I \\ I \end{bmatrix} V_{wo}^b \quad (43)$$

where  $u := [(\text{Ad}_{(g_d^{-1})} V_{wc}^b)^T \ u_e^T]^T$ . Let us define the error vector of the visual motion error system as

$$x := \begin{bmatrix} e_c^T & e_e^T \end{bmatrix}^T \quad (44)$$

which consists of the pose control error vector  $e_c$  and the estimation error vector  $e_e$ . It should be noted that if the vectors of the pose control error and the estimation one are equal to zero, then the actual relative rigid body motion  $g_{co}$  tends to the reference one  $g_d$  when  $x \rightarrow 0$ . It is noted that the visual motion error system (43) has block diagonal matrix with respect the input  $u$ , while the pose control error system was affected by the estimation input  $u_e$  in our previous work [6]. Next, we show an important relation between the input and the output of the visual motion error system.

**Lemma 2** *If  $V_{wo}^b = 0$ , then the visual motion error system (43) satisfies*

$$\int_0^T u^T(-x)dt \geq -\beta, \quad \forall T > 0 \quad (45)$$

where  $\beta$  is a positive scalar.

*Proof* Consider the following positive definite function

$$V = \frac{1}{2} \|p_{ec}\|^2 + \phi(e^{\hat{\xi}\theta_{ec}}) + \frac{1}{2} \|p_{ee}\|^2 + \phi(e^{\hat{\xi}\theta_{ee}}). \quad (46)$$

The positive definiteness of the function  $V$  results from the property of the error function  $\phi$ . Differentiating Eq. (46) with respect to time and using the skew-symmetry



Theorem 2 shows Lyapunov stability for the closed-loop system. If the camera velocity is decided directly, the control objective is achieved by using the proposed control law (49). Because a panoramic camera gives us a wide field of view, it is adequate to mobile robots. As for the visual motion error system with a panoramic camera, we have proposed the stabilizing control law based on the passivity. This is one of the main contributions of this research. Moreover, both the estimation and the control gain can be designed independently in the same framework. Although the dead angle problem [11] is not considered explicitly in this framework, our proposed method will overcome this problem by dealing with a collision avoidance as in [14]. Fig. 9 shows the pose controller for the panoramic camera. It should be noted that the desired image is not needed in the proposed controller which only entails the given desired relative rigid body motion  $g_d$  as shown in Fig. 9. Fig. 10 shows the block diagram of the closed-loop system which consists of the panoramic camera and the visual motion observer-based pose controller.

#### 4.4 $L_2$ -Gain Performance Analysis

In this subsection, we utilize  $L_2$ -gain performance analysis to evaluate the tracking performance of the control scheme in the presence of a moving target robot. The motion of the target robot is regarded as an external disturbance.

In order to derive a simple and practical gain condition, we redefine  $K_e = k_e I$  where  $k_e$  is a positive scalar.

**Theorem 3** *Given a positive scalar  $\gamma$ , assume*

$$k_{c,min} > \frac{\gamma^2(2k_e - 1) + 2(k_e - 1)}{2\{\gamma^2(2k_e - 1) - 1\}} \quad (51)$$

$$k_e > \frac{\gamma^2 + 1}{2\gamma^2} \quad (52)$$

where  $k_{c,min}$  means the minimum value in  $K_c$ . Then the closed-loop system (43) and (49) has  $L_2$ -gain  $\leq \gamma$ .

*Proof* Differentiating the positive definite function  $V$  defined in Eq. (33) along the trajectory of the closed-loop system yields

$$\begin{aligned} \dot{V} = & \frac{\gamma^2}{2} \|V_{wo}^b\|^2 - \frac{1}{2} \|x\|^2 - \frac{\gamma^2}{2} \|V_{wo}^b\|^2 + \frac{1}{2} \|x\|^2 \\ & - x^T u + x^T [\text{Ad}_{(e^{\hat{\xi}\theta_{ec}})}^T \text{Ad}_{(e^{\hat{\xi}\theta_{ee}})}^T]^T V_{wo}^b \end{aligned} \quad (53)$$

By completing the squares, we have

$$\begin{aligned} \dot{V} + \frac{1}{2} \|x\|^2 - \frac{\gamma^2}{2} \|V_{wo}^b\|^2 & = -\frac{\gamma^2}{2} \left\| V_{wo}^b - \frac{1}{\gamma^2} [\text{Ad}_{(e^{\hat{\xi}\theta_{ec}})}^T \text{Ad}_{(e^{\hat{\xi}\theta_{ee}})}^T] x \right\|^2 \\ & \quad + \frac{1}{2\gamma^2} \left\| [\text{Ad}_{(e^{\hat{\xi}\theta_{ec}})}^T \text{Ad}_{(e^{\hat{\xi}\theta_{ee}})}^T] x \right\|^2 - x^T u + \frac{1}{2} \|x\|^2 \\ & \leq \frac{1}{2\gamma^2} \|Wx\|^2 - x^T u + \frac{1}{2} \|x\|^2 \end{aligned} \quad (54)$$

where

$$W := \begin{bmatrix} I & \text{Ad}_{(e^{\hat{\xi}\theta_{ec}-\hat{\xi}\theta_{ee})}} \\ \text{Ad}_{(e^{\hat{\xi}\theta_{ec}-\hat{\xi}\theta_{ee})}}^T & I \end{bmatrix}.$$

Substituting the control input (49) into Eq. (54), we obtain

$$\dot{V} + \frac{1}{2}\|x\|^2 - \frac{\gamma^2}{2}\|V_{wo}^b\|^2 \leq -x^T P x \leq 0 \quad (55)$$

holds if  $P := K - \frac{1}{2\gamma^2}W - \frac{1}{2}I$  is positive semi-definite. Integrating Eq. (55) from 0 to  $T$  and noticing  $V(T) \geq 0$ , we have

$$\int_0^T \|x\|^2 dt \leq \gamma^2 \int_0^T \|V_{wo}^b\|^2 dt + 2V(0), \quad \forall T > 0. \quad (56)$$

From the Schur complement,

$$P = \begin{bmatrix} K_c - \frac{1}{2\gamma^2}I - \frac{1}{2}I & -\frac{1}{2\gamma^2}\text{Ad}_{(e^{\hat{\xi}\theta_{ec}-\hat{\xi}\theta_{ee})}} \\ -\frac{1}{2\gamma^2}\text{Ad}_{(e^{\hat{\xi}\theta_{ec}-\hat{\xi}\theta_{ee})}}^T & \left(k_e - \frac{1}{2\gamma^2} - \frac{1}{2}\right)I \end{bmatrix} \quad (57)$$

can be modified as the conditions (51)(52) in Theorem 3 by using  $\text{Ad}_{(e^{\hat{\xi}\theta_{ec}-\hat{\xi}\theta_{ee})}}^T \text{Ad}_{(e^{\hat{\xi}\theta_{ec}-\hat{\xi}\theta_{ee})}} = I$ .

The estimation gain does not have to be restricted to a scalar, although it causes slightly complicated gain conditions compared with Eqs. (51) and (52) for the reason that Schur complement can not be used. In this framework,  $\gamma$  can be considered as an indicator of the tracking performance.

*Remark 5* Our previous work has extended the eye-in-hand system with a pinhole camera to an eye-to-hand one which estimates both a robot hand and a target object [5]. In a similar way, this approach can be extended to estimate and control the poses of multi-robots by considering the fixed panoramic camera as surveillance systems which has it on the ceiling.

*Remark 6* For the  $L_2$ -gain performance analysis of the visual motion observer without the pose control, the following condition is only needed.

$$k_{e,min} > \frac{\gamma^2 + 1}{2\gamma^2} \quad (58)$$

where  $k_{e,min}$  means the minimum value in  $K_e$ .

## 5 Simulation and Experimental Results

Both the proposed estimation and control methods are confirmed by the simulation, while the experiment is carried out by using the proposed visual motion observer only.

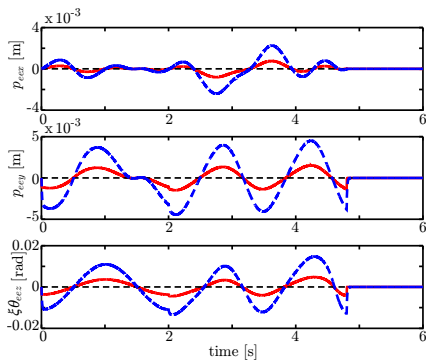


**Fig. 11** Estimation error  $e_e$  (Gain A: Dashed, Gain B: Solid).

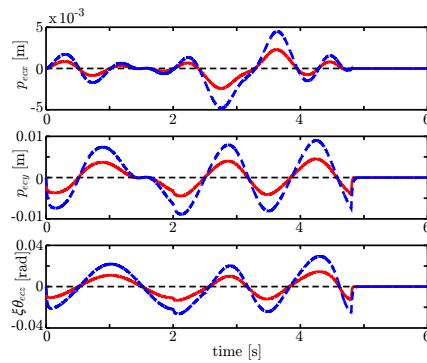


**Fig. 12** Pose control error  $e_c$  (Gain A: Dashed, Gain B: Solid).

### 5.1 Simulation Results

In this subsection, we present simulation results for stability and  $L_2$ -gain performance analysis in the case of a moving target robot. The target robot has four feature points and moves by  $t = 4.8$  [s]. The gains for the control law  $u$  (49) were empirically selected as follows:

- Gain A)  $\gamma = 0.123$ ,  $K_c = 50I$ ,  $k_e = 100$   
 Gain B)  $\gamma = 0.082$ ,  $K_c = 100I$ ,  $k_e = 300$ .

The simulation results are presented in Figs. 11 and 12 which illustrate the estimation error  $e_e$  and the pose control one  $e_c$ , respectively. In these figures, we focus on the errors of the translations of  $x$  and  $y$  and the rotation of  $z$ . In Figs. 11 and 12, the dashed line and the solid line are the errors in the case of  $\gamma = 0.123$  and  $\gamma = 0.082$ , respectively.

In the case of the static target robot, i.e., after  $t = 4.8$  [s], all errors in Figs. 11 and 12 tend to zero. Therefore, asymptotic stability can be confirmed through the simulation. In the presence of the moving target robot as disturbances by  $t = 4.8$  [s], the tracking performance is improved for the smaller values of  $\gamma$  from Figs. 11 and 12. Thus the simulation results show that  $L_2$ -gain is adequate for the performance measure of the visual motion observer-based pose control.

### 5.2 Experimental Results

In this subsection, we describe experimental results with respect to the proposed visual motion observer with a panoramic camera as shown in Fig. 13. A panoramic camera consists of a MTV-7310 camera and a hyperbolic mirror. In order to evaluate the estimation error exactly, the target object moves on the rail whose radius is 0.27 [m] as Fig. 13 with about 8.0 [s] per round instead of a target mobile robot. Fig. 14 is a captured image from the panoramic camera. The image feature points are acquired by OpenCV which is a library of programming functions for real time computer vision.

The experiment with respect to the stability analysis is carried out with an appropriate initial estimation error and the static target object. The experimental results are presented in Figs. 15 and 16. In Fig. 15, the dashed lines and the solid ones mean

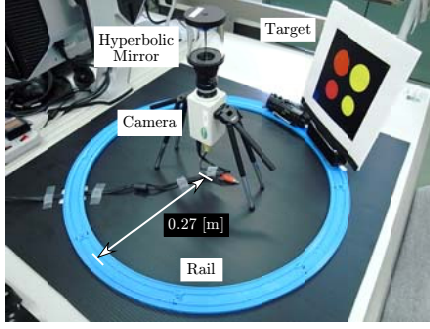


**Fig. 13** Panoramic camera and a target object.



**Fig. 14** Captured image from the panoramic camera.

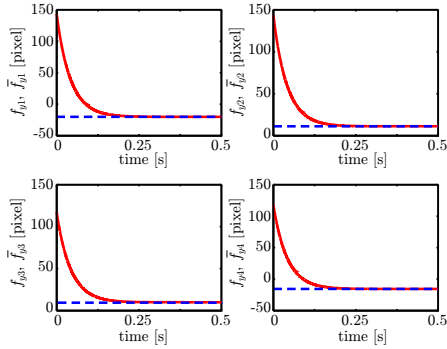


**Fig. 15** Image features and estimated ones w.r.t. the  $y$ -axis.

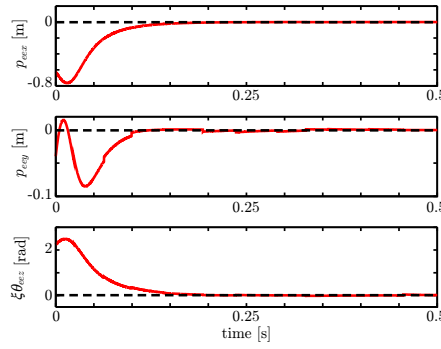


**Fig. 16** Estimation error  $e_e$  for the static target object with  $k_e = 10$ .

the image features and the estimated ones with respect to the  $y$ -axis, i.e.,  $f_{yi}$  and  $\hat{f}_{yi}$  ( $i = 1, \dots, 4$ ), respectively. The estimated image features coincide with the actual ones. From Fig. 16 which illustrates the estimation error of the translations of  $x$  and  $y$  and the rotation of  $z$ , we can confirm that the estimation error  $e_e$  tends to zero by using the proposed visual motion observer.

The experiments with respect to the  $L_2$ -gain performance analysis are carried out with the moving target object. We selected  $k_e = 1$  and  $k_e = 10$  as the estimation gain for  $\gamma = 1.001$  and  $\gamma = 0.230$ , respectively. Fig. 17 shows the estimation error  $e_e$ . The error in the case of  $k_e = 1$  and  $k_e = 10$  are shown in the left side and the right one of this figure. The estimation error is reduced for the smaller values of  $\gamma$  in Fig. 17. Fig. 18 depicts the estimated trajectory with  $k_e = 10$  and the course of the moving target object. The cross sign means the estimated value at both  $t = 0$  [s] and  $t = 8$  [s]. Because the average and the sample standard deviation of the norm of the estimated position from the origin  $\sqrt{\bar{p}_{mox}^2 + \bar{p}_{moy}^2}$  are  $0.269$  [m] and  $2.87 \times 10^{-3}$  [m], we can confirm that the estimated trajectory coincides with the ideal trajectory of the moving target object perfectly. It is the advantage of this research that the relative pose can be obtained by using only single panoramic camera in the around direction. The demonstration movie of the proposed visual motion observer can be seen on the Web site [19].

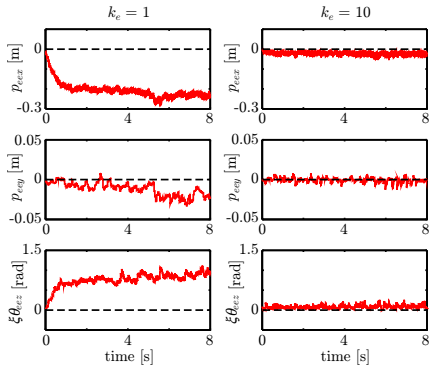


**Fig. 17** Estimation error  $e_e$  for the moving target object (left side: with  $k_e = 1$ ; right side: with  $k_e = 10$ )

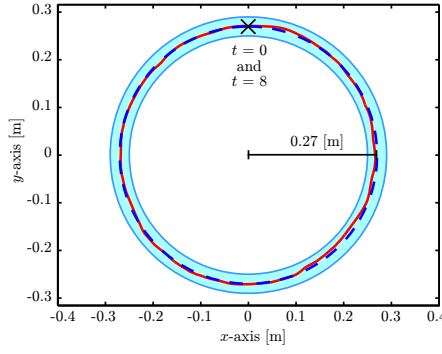


**Fig. 18** Estimated trajectory of the moving target object with  $k_e = 10$  (Ideal trajectory of the moving target object: Dashed, Estimated trajectory: Solid).

## 6 Conclusions

This paper proposes the visual motion observer and pose controller with a panoramic camera based on the passivity. The advantage of this research is that the relative pose between the leader and the follower robot can be obtained by using a single panoramic camera in our proposed method in the around direction. Especially, our proposed method does not need a desired image a priori. The estimation error system with a panoramic camera has the passivity which allows us to prove stability in the sense of Lyapunov. The visual motion error system which consists of the estimation error system and the pose control one preserves the passivity. As for the visual motion error system with a panoramic camera, we have proposed the stabilizing control law based on the passivity. This is one of the main contributions of this research. In the stabilizing control law, both the estimation and the control gain can be designed independently in the same framework. Our previous work [6] can be regarded as a special case of this study. Simulation results are presented to verify stability and  $L_2$ -gain performance in the visual motion observer-based pose control. Because the experiment is carried out by using the proposed visual motion observer only, we will realize pose control by using a mobile robot with the omnidirectional camera in the future work.

**Acknowledgements** We would like to thank Mr. Masahiro Matsuzawa in Kanazawa Institute of Technology for his effort to build experimental systems.

## A Notation of Homogeneous Transform

In this paper,  $p_{ab} = [x_{ab} \ y_{ab} \ z_{ab}]^T \in \mathcal{R}^3$  represents the position vector of origin of frame  $\Sigma_b$  from the origin of frame  $\Sigma_a$ . We use the notation  $e^{\hat{\xi}\theta_{ab}} \in \mathcal{R}^{3 \times 3}$  to represent the change of the principle axes of a frame  $\Sigma_b$  relative to a frame  $\Sigma_a$ .  $\xi_{ab} \in \mathcal{R}^3$  specifies the direction of rotation and  $\theta_{ab} \in \mathcal{R}$  is the angle of rotation. For simplicity we use  $\hat{\xi}\theta_{ab}$  to denote  $\hat{\xi}_{ab}\theta_{ab}$ . The notation ' $\wedge$ ' (wedge) is the skew-symmetric operator such that  $\hat{\xi}\theta = \xi \times \theta \mathbf{1}_3$  for the vector cross-product  $\times$  and any vector  $\theta \in \mathcal{R}^3$ . The notation ' $\vee$ ' (vee) denotes the inverse operator to ' $\wedge$ ', i.e.,  $so(3) \rightarrow \mathcal{R}^3$ . Recall that a skew-symmetric matrix corresponds to an axis of rotation

(via the mapping  $a \mapsto \hat{a}$ ). We use the  $4 \times 4$  matrix

$$g_{ab} = \begin{bmatrix} e^{\hat{\xi}\theta_{ab}} & p_{ab} \\ 0 & 1 \end{bmatrix} \quad (59)$$

as the homogeneous representation of  $g_{ab} = (p_{ab}, e^{\hat{\xi}\theta_{ab}}) \in SE(3)$  describing the configuration of a frame  $\Sigma_b$  relative to a frame  $\Sigma_a$ . The adjoint transformation associated with  $g_{ab}$  is denoted by

$$\text{Ad}_{(g_{ab})} = \begin{bmatrix} e^{\hat{\xi}\theta_{ab}} & \hat{p}_{ab}e^{\hat{\xi}\theta_{ab}} \\ 0 & e^{\hat{\xi}\theta_{ab}} \end{bmatrix}. \quad (60)$$

## References

1. F. Chaumette and S. A. Hutchinson, "Visual Servoing and Visual Tracking," In: B. Siciliano and O. Khatib (Eds), *Springer Handbook of Robotics*, Springer-Verlag, pp. 563–583 (2008)
2. V. Lippiello, B. Siciliano and L. Villani, "Position-Based Visual Servoing in Industrial Multirobot Cells Using a Hybrid Camera Configuration," *IEEE Trans. on Robotics*, Vol. 23, No. 1, pp. 73–86 (2007)
3. N. R. Gans and S. A. Hutchinson, "Stable Visual Servoing Through Hybrid Switched-System Control," *IEEE Trans. on Robotics*, Vol. 23, No. 3, pp. 530–540 (2007)
4. G. Hu, W. MacKunis, N. Gans, W. E. Dixon, J. Chen, A. Behal, and D. Dawson, "Homography-Based Visual Servo Control With Imperfect Camera Calibration," *IEEE Trans. on Automatic Control*, Vol. 54, No. 6, pp. 1318–1324 (2009)
5. H. Kawai, T. Murao and M. Fujita, "Passivity-based Dynamic Visual Feedback Control with Uncertainty of Camera Coordinate Frame," *Proc. of the 2005 American Control Conference* pp. 3701–3706 (2005)
6. M. Fujita, H. Kawai and M. W. Spong, "Passivity-based Dynamic Visual Feedback Control for Three Dimensional Target Tracking: Stability and  $L_2$ -gain Performance Analysis," *IEEE Trans. on Control Systems Technology*, Vol. 15, No. 1, pp. 40–52 (2007)
7. T. Murao, H. Kawai and M. Fujita, "Predictive Visual Feedback Control with Eye-in/to-Hand Configuration via Stabilizing Receding Horizon Approach," *Proc. of the 17th IFAC World Congress on Automatic Control*, pp. 5341–5346 (2008)
8. C. Geyer and K. Daniilidis, "A Unifying Theory for Central Panoramic Systems and Practical Implications," In: D. Vernon (Ed), *Computer Vision - ECCV 2000*, Springer-Verlag, pp. 445–461 (2000)
9. H. Hadj-Abdelkader, Y. Mezouar, N. Andreff and P. Martinet, "2 1/2D Visual Servoing with Central Catadioptric Cameras," *Proc. of the 2005 IEEE/RSJ International Conference on Intelligent Robots and Systems*, 2342–2347 (2005)
10. G. L. Mariottini and D. Prattichizzo, "EGT for Multiple View Geometry and Visual Servoing," *IEEE Robotics & Automation Magazine*, Vol. 12, No. 4, pp. 26–39 (2005)
11. R. T. Fomena and F. Chaumette, "Improvements on Visual Servoing From Spherical Targets Using a Spherical Projection Model," *IEEE Trans. on Robotics*, Vol. 25, No. 4, pp. 874–886 (2009)
12. A. K. Das, R. Fierro, V. Kumar, J. P. Ostrowski, J. Spletzer and C. J. Taylor, "A Vision-Based Formation Control Framework," *IEEE Trans. on Robotics and Automation*, Vol. 18, No. 5, pp. 813–825 (2002)
13. R. Vidal, O. Shakernia and S. Sastry, "Following the flock," *IEEE Robotics & Automation Magazine*, Vol. 11, No. 4, pp. 14–20 (2004)
14. M. Fujita, T. Hatanaka, N. Kobayashi, T. Ibuki and M. W. Spong, "Visual Motion Observer-based Pose Synchronization: A Passivity Approach," *Proc. of the 48th IEEE Conf. on Decision and Control and 28th Chinese Control Conf.*, pp. 2402–2407 (2009)
15. F. Chaumette, "Potential Problems of Stability and Convergence in Image-Based and Position-Based Visual Servoing," In: D. J. Kriegman, G. D. Hager, and A. S. Morse (Eds), *The Confluence of Vision and Control*, Springer-Verlag, pp. 66–78 (1998)
16. R. Murray, Z. Li and S. S. Sastry, *A Mathematical Introduction to Robotic Manipulation*, CRC Press (1994)
17. H. Michel and P. Rives, "Singularities in the Determination of the Situation of a Robot Effector from the Perspective View of 3 Points," *Technical Report*, INRIA (1993)

18. F. Bullo and A.D. Lewis, *Geometric Control of Mechanical Systems*, Springer-Verlag (2004)
19. <http://wwwr.kanazawa-it.ac.jp/kawai/research/VMO/movies.html>